

Kinetic Analysis of the Induction Period in Lipoxygenase Catalysis[†]

Maria J. Schilstra, Gerrit A. Veldink,* and Johannes F. G. Vliegthart

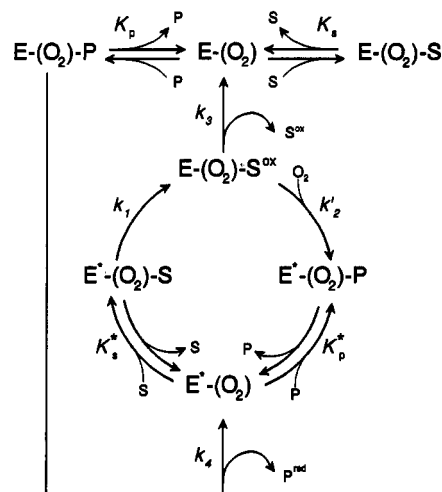
Bijvoet Center for Bio-Molecular Research, Department of Bio-Organic Chemistry, University of Utrecht, Padualaan 8, 3584 CH Utrecht, The Netherlands

Received March 9, 1993

ABSTRACT: The dioxygenation of 50 μM linoleate at 0.1 μM (13*S*)-hydroperoxylinoleate, 240 μM O_2 , pH 10, and 25 $^\circ\text{C}$, catalyzed by varying amounts of soybean lipoxygenase-1, was studied with rapid kinetic techniques. The aim was to assess the effect of transient redistributions of the Fe(II) and Fe(III) enzyme forms on the shape of the reaction progress curves. Reactions initiated with iron(II) lipoxygenase show an initial increase in rate, the “kinetic lag phase” or “induction period”. The duration of this induction period varies from approximately 1 s at [lipoxygenase] > 20 nM to 5 s at [lipoxygenase] = 3 nM. At [lipoxygenase] < 2 nM, the duration of the induction period in these curves is inversely proportional to [lipoxygenase]. The integrated steady-state rate equation for the single fatty acid binding site model of lipoxygenase catalysis [Schilstra et al. (1992) *Biochemistry* 31, 7692–7699] also shows an induction period whose duration is inversely proportional to [lipoxygenase]. These observations, in combination with non-steady-state numerical simulations, lead to the conclusion that, at [lipoxygenase] < 2 nM, pre-steady-state redistributions of enzyme intermediates occur fast with respect to the rate at which the concentrations of substrates and products change. At higher lipoxygenase concentrations, the pre-steady-state redistributions contribute significantly to the induction period. From a nonlinear least-squares fit to the steady-state rate equation of data obtained at lipoxygenase concentrations of 0.5 and 1 nM, it was calculated that 1% of the linoleate radicals that are formed after hydrogen abstraction dissociate from the active site before enzymic oxygen insertion has occurred.

Lipoxygenases (EC 1.13.11.12) catalyze dioxygenation of polyunsaturated fatty acids that contain one or more (1*Z*,4*Z*)-pentadiene systems. Their products are chiral (*E*,*Z*) conjugated hydroperoxy fatty acids (Veldink & Vliegthart, 1984; Schewe et al., 1986; Kühn et al., 1986a), which are the precursors of a number of physiological effectors in animal tissue (Parker, 1987) and possibly also in plants (Gardner, 1991).

Lipoxygenase catalysis of polyunsaturated fatty acid dioxygenation exhibits a characteristic “induction period” (Haining & Axelrod, 1958) or “kinetic lag phase” (Smith & Lands, 1972): after the initiation of the reaction, the rate gradually increases until a maximum rate is reached. In this paper, we shall refer to the phase in which the rate increases as the induction period, irrespective of the cause of the acceleration. The induction period is eliminated when the product hydroperoxide (P) (Scheme I) is present in micromolar amounts at the start of the reaction (Haining & Axelrod, 1958; Schilstra et al., 1992). EPR studies on soybean lipoxygenase-1 demonstrated that P converts the iron cofactor of lipoxygenase from Fe(II) into Fe(III) (De Groot et al., 1975a; Slappendel et al., 1983). However, initiation of the dioxygenation reaction with iron(III) instead of iron(II) lipoxygenase does not in general result in disappearance of the induction period. In some experiments (at 2.4 nM soybean lipoxygenase-1 and 0.24 or 0.48 mM linoleate) the progress curves of reactions initiated with iron(III) lipoxygenase seemed to be identical to those of reactions initiated with iron(II) lipoxygenase (De Groot et al., 1975b). When rapid kinetic techniques were used to study the initial stages of linoleate (23 or 86 μM) dioxygenation by 12 nM soybean lipoxygenase-

Scheme I^a

^a Abbreviations: E-(O₂) and E^{*}-(O₂), iron(II) and iron(III) lipoxygenase, equilibrium complexes with O₂; S, polyunsaturated fatty acid substrate; P, hydroperoxy fatty acid product; S^{ox} and P^{red}, oxidized and reduced forms of S and P (radical compounds); K_s, K_s^{*}, K_p, and K_p^{*}, equilibrium dissociation constants of E-S, E^{*}-S, E-P, and E^{*}-P; K_{oxy}, equilibrium dissociation constant of the lipoxygenase-oxygen complexes; k, rate constants; k'₂ = k₂/(1 + K_{oxy}/[O₂]).

1, a difference between the iron(II) and iron(III) lipoxygenase reactions was observed. The iron(II) lipoxygenase reaction started with a rate increase, but the iron(III) lipoxygenase reaction started with a burst (a decrease in rate). At 86 μM linoleate the burst was again followed by a rate increase (Schilstra et al., 1992). It was demonstrated that the mechanism in Scheme I (Ludwig et al., 1987; Schilstra et al., 1992) can, at least qualitatively, account for the initial acceleration in the iron(II) lipoxygenase curves and also for the burst followed by a rate increase in the iron(III) lipoxygenase reaction. In this mechanism, iron(III) lipoxy-

[†] M.J.S. is supported by a fellowship under European Community Science Programme Twinning Grant SC1-0197 to G.A.V., J.F.G.V., A. Finazzi-Agrò, and L. Avigliano.

* To whom correspondence should be addressed.

genase is the active enzyme form, because it is able to catalyze hydrogen abstraction from the polyunsaturated fatty acid (S) (Egmond et al., 1972; Egmond et al., 1973). Although oxygen insertion into the fatty acid radical may be a fast process, it is not immediate. Therefore, the fatty acid radical (S^{ox}) may occasionally dissociate from the active site, leaving inactive iron(II) lipoxygenase. Iron(II) lipoxygenase is converted back into iron(III) lipoxygenase by P.

In the present paper we shall demonstrate that this mechanism can also be used to explain the observations by De Groot et al. (1975b). We assess the contribution of pre-steady-state redistributions of iron(II) and iron(III) lipoxygenase to the duration of the induction period, from dioxygenation curves recorded at a range of lipoxygenase concentrations. We will show that the steady-state approach can be used to analyze dioxygenation data, provided these data are collected at sufficiently low lipoxygenase concentrations.

MATERIALS AND METHODS

Materials. The purification of soybean iron(II) lipoxygenase-1 and the preparation of (13*S*)-HPOD¹ ((13*S*)-hydroperoxy-(9*Z*,11*E*)-octadecadienoic acid) have been described previously (Finazzi-Agrò et al., 1973; Schilstra et al., 1992). The specific activity of the lipoxygenase preparation was 200 μmol min⁻¹ mg⁻¹. It was stored as a 17 mg/mL solution in AcB (0.05 M sodium acetate buffer, pH 5.5, containing 134 g/L ammonium sulfate). Chicken egg albumin (grade V) was obtained from Sigma. Linoleic acid ((9*Z*,12*Z*)-octadecadienoic acid; Janssen Chimica) was stored at -20 °C under argon as a 0.3 M solution in methanol pro analysi (Merck). The stock solution contained approximately 0.8% (mol/mol) racemic 9- and 13-HPOD (0.4% of each), formed by nonenzymic oxidation of linoleic acid as determined by reversed-phase HPLC. Iron(III) lipoxygenase was freshly prepared before each measurement by incubation of iron(II) lipoxygenase with an excess of (13*S*)-HPOD for approximately 15 min at room temperature. Typically 1.5 nmol of (13*S*)-HPOD was used to oxidize 1 nmol of iron(II) lipoxygenase in 200 μL of AcB.

Kinetic Measurements. Stopped-flow kinetic measurements were carried out as described by Schilstra et al. (1992). The concentrations of the various components after stopped-flow mixing were 10–80 μM linoleate, 0.01–7 μg/mL iron(II) or iron(III) lipoxygenase (0.1–70 nM), 0.03% methanol (v/v), and 0.5 mg/mL chicken egg albumin in BB10 (0.1 M sodium borate buffer, pH 10). The albumin was included in the reaction mixture to obtain reproducible results at all lipoxygenase concentrations (M. J. Schilstra et al., unpublished observations).

Data Collection and Processing. Reactions were recorded at 512 points per trace, and 10–15 traces were averaged to produce the final curves. Linoleate starting concentrations were estimated from the amount of 13-HPOD (P) formed after completion of the reaction. In order to estimate rates of product formation from the progress curves ([P] vs time), high-frequency noise was removed using a 25-point Fourier transform filter. A filter of this size gives good smoothing without distorting the overall shape of the curve. Points 1–12 and 501–512 were discarded from the smoothed curves. Product-formation rates r_i at time t_i were calculated from the

smoothed curves according to $r_i = ([P]_i - [P]_{i-1}) / (t_i - t_{i-1})$, where the index i indicates the i th point. Nonlinear least-squares fitting of data was carried out using the algorithm of Levenberg-Marquardt (Bevington, 1963).

Numerical Integration. Numerical integrations were performed as described in Schilstra et al. (1992).

Data Analysis. An analytical expression for the steady-state rate has been derived for the mechanism in Scheme I by Schilstra et al. (1992). This expression is given below, albeit in a slightly different form. The symbols are explained in the footnote to Scheme I. At a total lipoxygenase concentration $[e]$, the steady-state dioxygenation rate r_{ss} is given by

$$r_{ss} = V_{max}[S] / ((K_s^*(1 + [P]/K_p^*) + [S]) + \alpha(K_p(1 + [S]/K_s) + [P])[S]/[P]) \quad (1)$$

in which

$$V_{max} = \left(\frac{k_1}{k_3/k'_2 + 1} \right) [e] \quad (2)$$

$$\alpha = \frac{k_1/k_4}{k'_2/k_3 + 1} \quad (3)$$

$$k'_2 = k_2 / (1 + K_{oxy}/[O_2]) \quad (4)$$

Steady state is defined as a situation in which the various enzyme intermediates have reached constant concentrations. Steady state follows a pre-steady-state or transient phase, in which the enzyme species redistribute. Steady-state rate equations are derived for fixed concentrations of ligands (substrates, products, and inhibitors). During an enzymic reaction, ligand concentrations are continually changing, so that in general a steady-state approximation is not valid. However, if the rate at which the enzyme intermediates readjust to the changed conditions (i.e., the new ligand concentrations) is fast compared with the rate at which each ligand concentration changes, then the steady-state assumption is a good approximation. Since the ligand concentrations change at a rate that decreases with the enzyme concentration $[e]$, steady-state conditions are approached when $[e]$ approaches 0.

The integrated steady-state rate equation is sigmoid (Schilstra et al., 1992). The smaller the ratio k'_2/k_3 , the more pronounced the S-shape. Pre-steady-state interconversion of iron(II) and iron(III) lipoxygenase may, however, also affect the shape of the curves. Obviously, quantitative analysis of the curves using the steady-state rate equation is valid only when the effect of the pre-steady-state redistributions on the shape of the curves is negligible.

The steady-state rate, r_{ss} , is proportional to $[e]$: $r_{ss} = d[P]/dt = [e]f(S,P)$ (eq 1). The integrated steady-state rate equation is identical for all values of $[e]$, when it is expressed as a function of $t[e]$ ($\int dP/f(S,P) = t[e]$). When the effect of the transient redistributions is negligible, the duration of the induction period should be inversely proportional to $[e]$.

RESULTS

Effect of Enzyme Concentration on r_{max} . When dioxygenation of 50 μM linoleate was initiated with 0.1–70 nM iron(II) lipoxygenase, all reaction progress curves showed an initial increase in velocity and then proceeded at maximum velocity, r_{max} , for some time (see below). This maximum velocity was, within 5%, proportional to the enzyme concen-

¹ Abbreviations: HPOD, hydroperoxy-(9*Z*,11*E*)-octadecadienoic acid; 15-HETE, 15-hydroxyeicosa-(5*Z*,8*Z*,11*Z*,13*E*)-tetraenoic acid; AcB, 0.05 M sodium acetate buffer, pH 5.5, containing 134 g/L ammonium sulfate; BB10, 0.1 M sodium borate buffer, pH 10; HPLC, high-performance liquid chromatography.

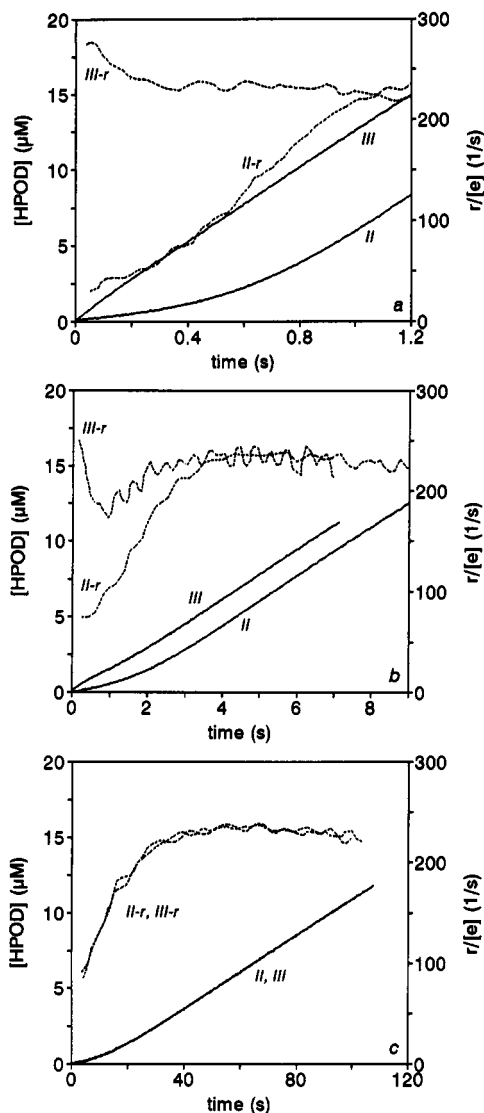


FIGURE 1: Dioxxygenation of 50 μM linoleate by 53 (a), 7 (b), and 0.53 nM lipoygenase (c). Solid lines (left vertical axis), progress curves, [13-HPOD] formed during reaction; dashed lines (curves II-r and III-r; right vertical axis), turnover rates, $r/[e]$ (tangents of the progress curves). Reactions were started with either iron(II) lipoygenase (curves II) or iron(III) lipoygenase (curves III).

tration, $[e]$. Weighted linear regression yielded a 0 intercept and a slope of $230 \pm 10 \text{ s}^{-1}$.

Effect of Enzyme Concentration on the Shape of the Progress Curves. The initial stages of the dioxxygenation of 50 μM linoleate (containing approximately 0.4 μM racemic 9- and 13-HPOD), initiated with three different concentrations of either iron(II) or iron(III) lipoygenase, are shown in Figure 1. The turnover rates, $r/[e]$, calculated from the progress curves, are plotted in the same graphs. The full time scales in the plots were set to values inversely proportional to the enzyme concentrations in order to facilitate comparison.

At an enzyme concentration of 53 nM (Figure 1a), the progress curves of reactions initiated with iron(II) lipoygenase are completely different from the curves of reactions that were initiated with iron(III) lipoygenase. The reaction started with iron(II) lipoygenase has a pronounced induction period. The maximum rate is reached 1.1 s after the start of the reaction. In 1.4 s 10 μM HPOD is produced, and the induction period covers 75% of this period. The initial rate in the reaction started with iron(III) lipoygenase is high (approximately 280 s^{-1}), but it decreases within 0.5 s to 230

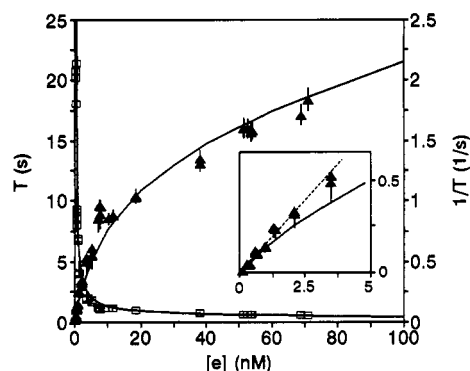


FIGURE 2: The effect of enzyme concentration on the duration of the lag period. Dioxxygenation of 50 μM linoleate was initiated with varying amounts of iron(II) lipoygenase. T is the intercept on the time axis of a straight line through the portion of the reaction progress curve where the rate is maximal. Data are plotted as T (squares, left vertical axis) and as $1/T$ (triangles, right vertical axis). Solid lines: simulated data with $k_1 = 300$, $k_4 = 150 \text{ s}^{-1}$, $k_2/k_3 = 200$, $K^* = 8 \mu\text{M}$, $K_p^* = 25 \mu\text{M}$, $K_s = 20 \mu\text{M}$, $K_p = 15 \mu\text{M}$, $K_{\text{oxy}} = 100 \mu\text{M}$, and O_2 , linoleate, and HPOD starting concentrations of 240, 50, and 0.1 μM , respectively. Inset: detail of $1/T$ vs $[e]$ curve; dashed line, $1/T$ vs $[e]$ for steady-state simulations; slope, $0.18 \text{ nM}^{-1} \text{ s}^{-1}$.

s^{-1} . The rate then stays constant for nearly 0.5 s, and 1 s after the start of the reaction it begins to decrease further.

At lower enzyme concentrations, the contribution of the induction period to the full curve in the reactions started with iron(II) lipoygenase becomes smaller, and the iron(III) lipoygenase curves begin to show a rate increase after the initial decrease. At $[e] = 7 \text{ nM}$ (Figure 1b), the maximum rate is reached after approximately 3.5 s, which is only half of the time required to produce 10 μM HPOD. The rate of the reaction started with 7 nM iron(III) lipoygenase has a clear minimum at 1 s and reaches a maximum after 3.5 s.

At very low enzyme concentrations ($< 3 \text{ nM}$), the iron(II) and iron(III) lipoygenase curves are very similar. The iron(II) lipoygenase curves still show an initial increase in rate. In the iron(III) lipoygenase curves, the relative contribution of the burst is small, but the rate increase following the initial decrease is more apparent. Below $[e] \approx 2 \text{ nM}$, the contribution of the induction period to the full iron(II) lipoygenase curves seems to remain constant. At these low enzyme concentrations, the amount of HPOD produced during the burst period in the iron(III) lipoygenase curves is smaller than the experimental error. As a result, the progress curves of the reactions initiated with iron(II) and iron(III) lipoygenase coincide (Figure 1c).

Duration of the Induction Period. In order to study the duration of the induction period as a function of the enzyme concentration more precisely, we recorded oxygenation curves at a starting substrate concentration of 50 μM linoleate for a range of lipoygenase concentrations (0.1–70 nM). We use the quantity T to quantify the duration of the induction period. T is defined as the time axis intercept of a straight line through the portion of the reaction progress curve where the rate is maximal. T is introduced because it is more accurately measurable than the exact point where the rate has become maximal. The rate becomes maximal at $2\text{--}3T$. In certain enzymic reactions, those with a strictly exponential relaxation toward the steady state, T is equal to τ , the lifetime of the transient state (Gutfreund, 1965). However, in the lipoygenase reaction, T is not equal to τ , as will be pointed out below.

In Figure 2, T is plotted as a function of $[e]$. At low $[e]$ the values of T decrease strongly, from 60 s at $[e] = 0.1 \text{ nM}$ to 1 s at $[e] = 7 \text{ nM}$, but in the range $[e] = 10\text{--}90 \text{ nM}$, T only decreases from 1 to 0.55 s. All curves recorded at $[e] < 2 \text{ nM}$

coincide when plotted as a function of $t/[e]$. A plot of $1/T$ against $[e]$ (Figure 2) shows that $1/T$ is linearly related to $[e]$ at $[e] < 2$ nM (inset). Linear regression of the data gives a slope of $0.16 \pm 0.1 \text{ s}^{-1} \text{ nM}^{-1}$. Above $[e] = 3$ nM, the values of $1/T$ begin to deviate from the straight line.

Numerical Simulations. We carried out numerical simulations of the oxygenation process at various enzyme concentrations, in order to investigate whether the observed relation between T and $[e]$ is in agreement with the proposed mechanism (Scheme 1). The solid lines in Figure 2 are the result of simulations in which the following parameter values were used: $k_1 = 300 \text{ s}^{-1}$ (Egmond et al., 1976; Verhagen et al., 1978; Schilstra et al., 1992; see also below), $k_4 = 150 \text{ s}^{-1}$ (Aoshima et al., 1977; Verhagen et al., 1978), $K_s^* = 8 \text{ } \mu\text{M}$ (Schilstra et al., 1992; see also below), $K_p^* = 25 \text{ } \mu\text{M}$ (Schilstra et al., 1992), $K_p = 15 \text{ } \mu\text{M}$ (Aoshima et al., 1977), and $K_{\text{oxy}} = 100 \text{ } \mu\text{M}$ [estimated from data in Egmond et al., (1976)]. The starting $[S]$ was $50 \text{ } \mu\text{M}$. In the $50 \text{ } \mu\text{M}$ linoleate solutions that we used in the experiments, the total concentration of HPOD was $0.4 \text{ } \mu\text{M}$ (see Materials and Methods). In our analysis we have assumed that (13S)-HPOD, one-fourth of all HPOD present, is the only HPOD species capable of oxidizing iron(II) lipoxygenase. Therefore, the simulations were started with $[P] = 0.1 \text{ } \mu\text{M}$. We performed integrations with K_s values from 5 to $50 \text{ } \mu\text{M}$. Since K_s and k'_2/k_3 are strongly correlated (see Estimation of k'_2/k_3 , below), the value of K_s fixes the value of k'_2/k_3 . A good agreement between the observed and simulated data was obtained with $K_s = 20 \text{ } \mu\text{M}$ and $k'_2/k_3 = 140$ (solid lines in Figure 2). The duration of the simulated induction periods appeared to be strongly dependent on the initial $[P]$. The assumption that only (13S)-HPOD can oxidize iron(II) lipoxygenase is based on observations by De Groot et al. (1975b) and Verhagen et al. (1977) on (9R)- and (13R)-HPOD. There are no data on (9S)-HPOD, however. Therefore, we have also carried out the simulations with an initial $[P] = 0.2 \text{ } \mu\text{M}$. With $k'_2/k_3 = 230$, $K_s = 10 \text{ } \mu\text{M}$, and all other parameters as above, the plot of simulated T vs $[e]$ was very similar to the one obtained for an initial $[P] = 0.1 \text{ } \mu\text{M}$, $k'_2/k_3 = 140$, and $K_s = 20 \text{ } \mu\text{M}$.

Numerical integration of the steady-state equations was also carried out with the parameters mentioned above. The value of T for the integrated steady-state equation (T_{ss}) at $[e] = 1$ nM is 5.6 s. Since T_{ss} is inversely proportional to $[e]$ (by definition; see Materials and Methods), the slope of the plot of $1/T_{ss}$ against $[e]$ is 0.18 s^{-1} . This value is in good agreement with the experimental slope of $1/T$ vs $[e]$ at $[e] < 2$ nM: 0.16 s^{-1} (see above).

The simulations provide information on the effect of enzyme concentration on the process of iron(II) and iron(III) lipoxygenase redistribution. This process is rather complex, because the effect of changing $[P]/[S]$ is twofold. With increasing $[P]/[S]$, the oxidation of iron(II) lipoxygenase proceeds more rapidly, so that the lifetime, τ , of the transient state decreases. In addition, the steady-state fraction of iron(III) lipoxygenase, $([e^*]/[e])_{inf}$, to which the system relaxes, also increases with increasing $[P]/[S]$. In order to study the transient state separately, we carried out simulations in which $[S]$ and $[P]$ were kept constant. At constant $[S]$ and $[P]$, the redistribution of iron(II) and iron(III) lipoxygenase can be described as a single-exponential process. This process is independent of $[e]$ and the initial distribution of enzyme species, provided $[e]$ is small with respect to the ligand concentrations. Figure 3a shows that the lifetime of the transient state decreases rapidly, from 0.52 to 0.1 s, when $[P]$ increases from 0.1 to $3 \text{ } \mu\text{M}$. At $[P] = 20 \text{ } \mu\text{M}$ and $[S] = 30 \text{ } \mu\text{M}$, τ is less than 0.02 s. The value

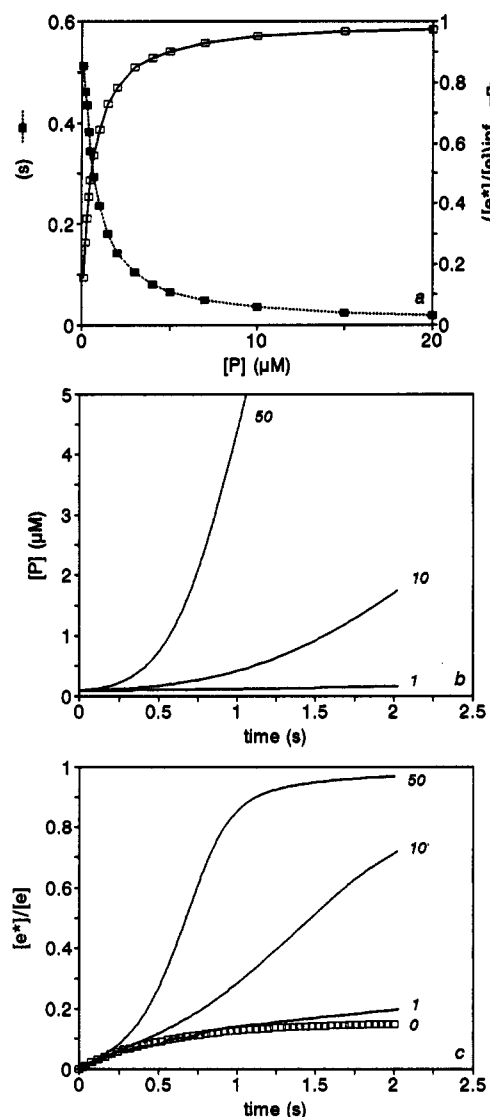


FIGURE 3: Simulated lipoxygenase reaction; parameters are as in Figure 2. Panel a: simulations at constant $[S]$, $[P]$, and $[O_2]$; $[O_2] = 240 \text{ } \mu\text{M}$, $[S] + [P] = 50.1 \text{ } \mu\text{M}$. The graph shows the effect of $[P]$ on the lifetime, τ , of the transient state (closed squares, left vertical axis) and on the steady-state fraction of iron(III) lipoxygenase ($[e^*]/[e]_{inf}$) (e^* indicates iron(III) lipoxygenase) (open squares, right vertical axis). Panels b and c: simulations in which $[S]$, $[P]$, and $[O_2]$ were allowed to vary. Starting $[S]$, $[P]$, and $[O_2]$: 50, 0.1, and $240 \text{ } \mu\text{M}$, respectively. The graphs show the initial 2 s of dioxygenation reactions at total enzyme concentrations $[e] = 1, 10,$ and 50 nM (curves 1, 10, and 50). (a) $[P]$. (b) Fraction of iron(III) lipoxygenase $[e^*]/[e]$ during the reaction (non-steady state). Curve 0 (open squares): fraction of iron(III) lipoxygenase in a simulation at constant $[S]$, $[P]$, and $[O_2]$.

of $([e^*]/[e])_{inf}$ increases from 0.15 ($[P] = 0.1 \text{ } \mu\text{M}$) to 0.85 ($[P] = 3 \text{ } \mu\text{M}$) and further to 0.97 ($[P] = 20 \text{ } \mu\text{M}$). The simulated curve for $[P] = 0.1$, $[S] = 50 \text{ } \mu\text{M}$, and an initial $[e^*]/[e] = 0$ is shown in Figure 3c (curve 0).

In simulations in which $[P]$ and $[S]$ are allowed to vary, the increase of $[e^*]/[e]$ is nonexponential owing to the effects of changing $[P]/[S]$. During the initial 2 s of a reaction at $[e] = 1$ nM, $[P]$ only increases from 0.1 to $0.16 \text{ } \mu\text{M}$ and the increase in $[e^*]/[e]$ is still close to exponential. At $[e] = 10$ nM, however, $[P]$ increases in 1 s from 0.1 to $1.7 \text{ } \mu\text{M}$, and at $[e] = 50$ nM, $[P]$ increases to $15 \text{ } \mu\text{M}$ (Figure 3b). There is a concomitant decrease in the lifetime of the transient state, but $([e^*]/[e])_{inf}$ increases, and the result is an S-shaped curve (Figure 3c).

Estimation of k'_2/k_3 . The observations on the duration of the induction period, combined with the numerical simulations, suggest that a steady-state approximation of the data is valid at enzyme concentrations below approximately 2 nM. At higher enzyme concentrations, transient processes begin to affect the shape of the reaction progress curves and in particular the duration of the induction period. Therefore, the steady-state rate equation (eq 1) may be used to estimate the value of k'_2/k_3 from curves recorded at enzyme concentrations smaller than 2 nM. We measured the dioxygenation of 13, 27, 39, 52, and 83 μM linoleate for a period of 50–200 s. The reactions were initiated with 0.5 or 1.0 nM iron(II) lipoxygenase. The inverse relationship between T and $[e]$ held at each linoleate concentration. Rates were calculated from the smoothed progress curves (see Materials and Methods) and expressed as a function of $[\text{HPOD}]$ and $[\text{linoleate}]$. Five or six equally spaced data points per curve were fitted to the steady-state rate equation (it should be noted that, according to Cornish-Bowden (1972), even as few as five or six data points taken from a single curve are statistically not completely independent; therefore, estimates of the precision of the parameters may be inaccurate). The variation of $[\text{HPOD}]/K^*_p$, $[\text{linoleate}]/K_s$, $[\text{HPOD}]/K_p$, and $[\text{O}_2]/K_{\text{O}_2}$ in these data is too small to provide statistically significant estimates of K^*_p , K_s , K_p , and K_{O_2} . Therefore, K^*_p , K_p , and K_{O_2} were entered as constants (25, 15, and 100 μM , respectively; Schilstra et al., 1992; Aoshima et al., 1977; Egmond et al., 1976). $[\text{O}_2]$ was assumed to be 240 μM throughout the curves, because at $K_{\text{O}_2} = 100 \mu\text{M}$, a decrease of $[\text{O}_2]$ from 240 to 220 μM only results in a decrease of k'_2/k_3 of 2.6%. The values obtained for $V_{\text{max}}/[e]$ and K^*_s were $300 \pm 5 \text{ s}^{-1}$ and $7.5 \pm 0.5 \mu\text{M}$, respectively, independent of the other parameters. A range of constant values was entered for K_s , since no published value is available. The best-fit value of α (eq 3) is related to the input value of K_s : if $K_s = 5 \mu\text{M}$, then $\alpha = 0.0049 \pm 0.0003$; if $K_s = 25 \mu\text{M}$, then $\alpha = 0.017 \pm 0.001$. All K_s values gave an equally good fit, but the agreement between the observed and simulated values of T (see above; Figure 2) was best at $K_s = 20$ and $\alpha = 0.014$. In Figure 4 a comparison is shown of the experimental data and the calculated curves for $V_{\text{max}} = 300 \text{ s}^{-1}$, $K^*_s = 10 \mu\text{M}$, $K^*_p = 25 \mu\text{M}$, $K_s = 20 \mu\text{M}$, $K_p = 15 \mu\text{M}$, $K_{\text{O}_2} = 100 \mu\text{M}$, and $\alpha = 0.014$, projected on the $[\text{HPOD}]$ (4a) and $[\text{linoleate}]$ (4b) axes.

The value of k'_2/k_3 may be calculated from the best-fit values of $V_{\text{max}}/[e]$ (300 s^{-1}) and α (0.014) using eqs 2 and 3. If $k_4 = 150 \text{ s}^{-1}$ and $K_{\text{O}_2} = 100 \mu\text{M}$, then $k'_2/k_3 = 140$ and $k_2/k_3 = 200$.

DISCUSSION

The origin of the induction period in the lipoxygenase-catalyzed dioxygenation of polyunsaturated fatty acids has been the subject of much discussion. In particular, the finding that initiating the dioxygenation of 240 or 480 μM linoleate with iron(III) instead of iron(II) lipoxygenase did not eliminate the induction period (De Groot et al., 1975b) seemed to be inconsistent with the theory that iron(III) lipoxygenase is the active enzyme species (De Groot et al., 1975a; Slappendel et al., 1983). Many authors were tempted to speculate about the need for a second activation step in the kinetic scheme and regulatory functions of substrates and products [e.g., De Groot (1975b), Lagocki et al. (1976), Egmond et al. (1977), and Schewe et al. (1986)]. The results of the present study, however, strongly support the idea that the sigmoid shape of the progress curves can be explained within the kinetic model presented in Scheme I, without any further assumptions.

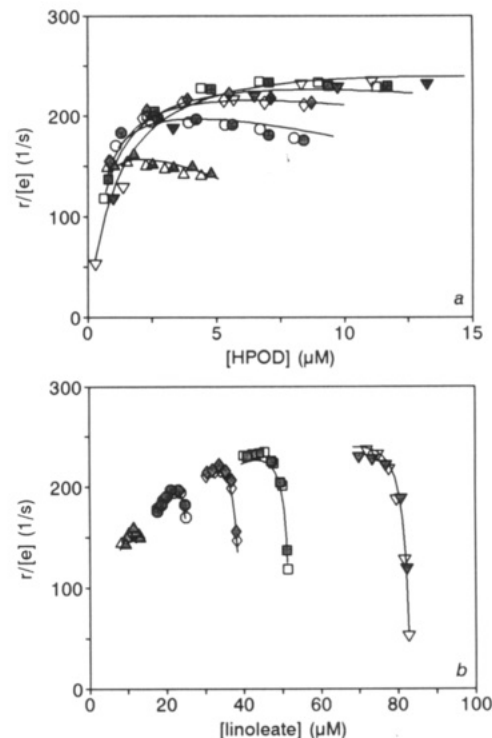


FIGURE 4: Steady-state turnover rates at various linoleate and 13-HPOD concentrations, obtained from smoothed dioxygenation curves, projected on the $[\text{13-HPOD}]$ (a) or $[\text{linoleate}]$ axis (b). Dioxygenation of 13, 27, 39, 52, and 83 μM linoleate was initiated with 0.5 (closed symbols) or 1.0 nM iron(II) lipoxygenase (open symbols). The solid lines represent the best nonlinear least-squares fit of the data with eq 1 (see text). Parameter values: $V_{\text{max}}/[e] = 300 \text{ s}^{-1}$, $K^*_s = 8 \mu\text{M}$, $K^*_p = 25 \mu\text{M}$, $K_s = 20 \mu\text{M}$, $K_p = 15 \mu\text{M}$, and $\alpha = 0.014$.

In reactions at $[e] > 20 \text{ nM}$, the ligand concentrations, and in particular $[\text{P}]$, change very rapidly with respect to the rate at which iron(II) and iron(III) lipoxygenase interconvert. As a consequence, the discrepancy between the actual distribution of enzyme species and the theoretical steady-state distribution is very large. At these high enzyme concentrations, reactions initiated with iron(II) lipoxygenase and reactions initiated with iron(III) lipoxygenase progress in a completely different way. The iron(II) lipoxygenase curves start with a relatively long induction period, whereas the iron(III) lipoxygenase curves show an initial burst of hydroperoxide production.

In contrast, at $[e] < 2 \text{ nM}$ the rate at which the transient redistributions take place is fast with respect to the dioxygenation rate. Reactions initiated with either iron(II) or iron(III) lipoxygenase show an induction period, whose duration (quantified by T) is inversely proportional to $[e]$. This reciprocal relationship between T and $[e]$ is not unique for this system. A similar inverse proportionality can be calculated from data on the oxygenation of arachidonic acid by soybean lipoxygenase (Smith & Lands, 1972). The reciprocity of T and $[e]$ suggests that transient redistributions are so fast that they do not affect T (see Materials and Methods). Owing to the low reaction rate, $[\text{P}]$ changes very little during the transient phase, even when the reaction is initiated with iron(III) lipoxygenase. Under these conditions, the difference between the iron(II) and iron(III) lipoxygenase curves is too small to be detected, and the curves coincide. This explains the observations of De Groot et al. (1975b; see above). Numerical simulations indicate that the differences between the non-steady-state and steady-state curves are very small indeed. Hence, a steady-state approximation of the data is justified at these low enzyme concentrations.

In summary: The sigmoid shape of the dioxygenation progress curve predicted by integration of the steady-state rate equation reveals itself in reaction progress curves obtained at low lipoxygenase concentrations. Here the initial acceleration is mainly due to the fact that the steady-state distribution of active iron(III) and inactive iron(II) lipoxygenase is dependent on $[P]/[S]$. At high lipoxygenase concentrations redistribution of enzyme species is slow with respect to the rate at which $[P]$ and $[S]$ change. The system approaches the steady state very late in the reaction. At high $[e]$, the initial increase in rate in reactions initiated with iron(II) lipoxygenase is mainly transient in character.

The duration of the induction period, at both high and low $[e]$, is determined largely by the initial ratio $[S]/[P]$. Decreasing $[P]$ will increase T , and the reaction will not proceed at all in the absence of P . This is in agreement with the observations of Smith and Lands (1972), who reported that reduction of P by the glutathione/glutathione peroxidase system increases the duration of the induction period. At high peroxidase concentrations, they found no detectable reaction.

The duration of the induction period is related to the efficiency of the dioxygenation reaction: the larger the fraction of S^{ox} radicals that dissociate from the active site before oxygen insertion has occurred, the longer the induction period. It was estimated by fitting rates obtained at low $[e]$ to the steady-state rate equation that the number of radicals that undergo enzymic oxygen insertion is, at $[O_2] = 240 \mu M$, 2 orders of magnitude larger than the number of radicals that dissociate from the enzyme. Kühn et al. (1986b) determined that in the dioxygenation of (15S)-HETE by reticulocyte lipoxygenase, 1 mol of hydroperoxy fatty acid is consumed during the dioxygenation of 9 mol of (15S)-HETE. Linoleate dioxygenation catalysis by soybean lipoxygenase-1 is thus 10 times as efficient. Soybean lipoxygenase-1 is also a more efficient catalyst than other soybean lipoxygenases. It has been observed that the induction period in lipoxygenase-2-catalyzed dioxygenation of linoleate is 10 times longer than than in lipoxygenase-1-catalyzed reactions with the same r_{max} (M. J. Schilstra et al., unpublished observations). In the lipoxygenase-2 reaction also substantial amounts of oxodienes are formed. These oxodienes are indicative of the consumption of HPOD by iron(II) lipoxygenase and thus of S^{ox} radicals that have dissociated from the enzyme before the oxygen insertion step.

Notwithstanding its relatively high efficiency, soybean lipoxygenase-1, working at a turnover rate of $150 s^{-1}$, would lose over 95% of its activity in 2 to 3 s if some of its reaction product (1%) were not used to convert the inactive Fe(II) enzyme into the active Fe(III) form.

ACKNOWLEDGMENT

We thank Dr. N. C. Millar (King's College, University of London) for providing the simulation program KSIM (Gear

method for numerical integration) and Dr. S. R. Martin (National Institute for Medical Research, London) for helpful discussions.

REFERENCES

- Aoshima, H., Kajiwara, T., Hanataka, A., Nakatani, H., & Hiromi, K. (1977) *Biochim. Biophys. Acta* 486, 121–126.
- Bevington, P. R. (1969) in *Data Reduction and Error Analysis for the Physical Sciences*, McGraw-Hill, New York.
- Cornish-Bowden, A. (1972) *Biochem. J.* 130, 637–639.
- De Groot, J. J. M., Veldink, G. A., Vliegthart, J. F. G., Bolding, R., Wever, R., & Van Gelder, B. F. (1975a) *Biochim. Biophys. Acta* 377, 71–79.
- De Groot, J. J. M., Garssen, G. J., Veldink, G. A., Vliegthart, J. F. G., Bolding, J., & Egmond, M. R. (1975b) *FEBS Lett.* 56, 50–54.
- Egmond, M. R., Vliegthart, J. F. G., & Bolding, J. (1972) *Biochem. Biophys. Res. Commun.* 48, 1055–1060.
- Egmond, M. R., Veldink, G. A., Vliegthart, J. F. G., & Bolding, J. (1973) *Biochim. Biophys. Acta* 326, 279–284.
- Egmond, M. R., Brunori, M., & Fasella, P. M. (1976) *Eur. J. Biochem.* 61, 93–100.
- Egmond, M. R., Fasella, P., Veldink, G. A., Vliegthart, J. F. G., & Bolding, J. (1977) *Eur. J. Biochem.* 76, 469–479.
- Finazzi-Agrò, A., Avigliano, L., Veldink, G. A., Vliegthart, J. F. G., & Bolding, J. (1973) *Biochim. Biophys. Acta* 326, 462–470.
- Gardner, H. W. (1991) *Biochim. Biophys. Acta* 1084, 221–239.
- Gutfreund, H. (1965) in *An Introduction to the Study of Enzymes* pp 50–61, Blackwell, Oxford, U.K.
- Haining, J. L., & Axelrod, B. (1958) *J. Biol. Chem.* 232, 193–202.
- Kühn, H., Schewe, T., & Rapoport, S. M. (1986a) *Adv. Enzymol. Relat. Areas Mol. Biol.* 58, 273–311.
- Kühn, H., Wiesner, H., Schewe, T., Lankin, V. Z., Nekrasov, A., & Rapoport, S. M. (1986b) *FEBS Lett.* 203, 247–252.
- Lagocki, J. W., Emken, E. A., Law, J. H., & Kézdy, F. (1976) *J. Biol. Chem.* 254, 6001–6006.
- Ludwig, P., Holzhütter, H.-G., Colosimo, A., Silvestrini, M. C., Schewe, T., & Rapoport, S. M. (1987) *Eur. J. Biochem.* 168, 325–337.
- Parker, C. W. (1987) *Annu. Rev. Immunol.* 5, 65–84.
- Schewe, T., Rapoport, S. M., & Kühn, H. (1986) *Adv. Enzymol. Relat. Areas Mol. Biol.* 58, 191–272.
- Schilstra, M. J., Veldink, G. A., Verhagen, J., & Vliegthart, J. F. G. (1992) *Biochemistry* 31, 7692–7699.
- Slappendel, S., Veldink, G. A., Vliegthart, J. F. G., Aasa, R., & Malmström, B. G. (1983) *Biochim. Biophys. Acta* 747, 32–36.
- Smith, W. L., & Lands, W. E. M. (1972) *J. Biol. Chem.* 247, 1038–1047.
- Veldink, G. A., & Vliegthart, J. F. G. (1984) in *Advances in Inorganic Biochemistry* (Eichhorn, G. L., & Marzili, L. G., Eds.) Vol. VI, pp 139–161, Elsevier, Amsterdam.
- Verhagen, J., Bouman, A. A., Vliegthart, J. F. G., & Bolding, J. (1977) *Biochim. Biophys. Acta* 486, 114–120.
- Verhagen, J., Veldink, G. A., Egmond, M. R., Vliegthart, J. F. G., & Bolding, J., & Van der Star, J. (1978) *Biochim. Biophys. Acta* 529, 369–379.